



1 Biogeochemical and plant trait mechanisms drive enhanced methane emissions
2 in response to whole-ecosystem warming

3

4 Genevieve L. Noyce and J. Patrick Megonigal

5 Smithsonian Environmental Research Center, Edgewater, MD

6

7 Corresponding author: G. Noyce, noyceg@si.edu, 443-482-2351

8

9

10

11

12

13

14

15

16

17

18

19

20

21

22

23

24

25

26



27 **Abstract**

28 Climate warming perturbs ecosystem carbon (C) cycling, causing both positive and negative
29 feedbacks on greenhouse gas emissions. In 2016, we began a tidal marsh field experiment in two
30 vegetation communities to investigate the mechanisms by which whole-ecosystem warming alters C gain,
31 via plant-driven sequestration in soils, and C loss, primarily via methane (CH₄) emissions. Here, we
32 report the results from the first four years. As expected, warming of 5.1 °C more than doubled CH₄
33 emissions in both plant communities. We propose this was caused by a combination of four mechanisms:
34 (i) a decrease in the proportion of CH₄ consumed by CH₄ oxidation, (ii) more C substrates available for
35 methanogenesis, (iii) reduced competition between methanogens and sulfate reducing bacteria, and (iv)
36 indirect effects of plant traits. Plots dominated by *Spartina patens* consistently emitted more CH₄ than
37 plots dominated by *Schoenoplectus americanus*, indicating key differences in the roles these common
38 wetland plants play in affecting anaerobic soil biogeochemistry and suggesting that plant composition can
39 modulate coastal wetland responses to climate change.

40

41 **1. Introduction**

42 Methane (CH₄) is a potent greenhouse gas that contributes to 15-19 % of total greenhouse gas
43 radiative forcing (IPCC, 2013) and has a sustained-flux global warming potential that is 45 times that of
44 CO₂ on a 100-year timescale (Neubauer & Megonigal, 2015). Wetlands are the largest natural source of
45 CH₄ to the atmosphere and were recently identified as the largest source of uncertainty in the global CH₄
46 budget (Saunio et al., 2016). Recent estimates calculate that CH₄ emissions from vegetated coastal
47 wetlands offset 3.6 of the 12.2 million metric tons (MMT) of CO₂ equivalents accumulated by these
48 ecosystems each year (EPA, 2017). Despite this, there is still a substantial knowledge gap regarding how
49 global change factors, such as climate warming, will alter coastal wetland CH₄ emissions (Mcleod et al.,
50 2011) even though these feedbacks have the potential to shift coastal wetlands from being a net sink of C
51 to a net source (Al-Haj & Fulweiler, 2020; Bridgham et al., 2006).



52 The net flux of CH₄ to the atmosphere from any ecosystem represents the balance between the
53 amount of CH₄ produced (methanogenesis), the amount of CH₄ oxidized (methanotrophy), and the rate of
54 CH₄ transport from the soil. Rates of methanogenesis are driven by low redox conditions and substrate
55 availability, while aerobic CH₄ oxidation requires both O₂ and CH₄ as substrates. Roots and rhizomes in
56 wetland ecosystems influence methane-related substrates through at least two mechanisms: (i) deposition
57 of organic compounds that support multiple pathways of heterotrophic microbial respiration, including
58 methanogenesis, and (ii) release of O₂ that simultaneously promotes CH₄ oxidation (Philippot et al., 2009;
59 Stanley & Ward, 2010) and regeneration of competing electron acceptors such as Fe(III) and SO₄. Root
60 exudates, which typically include low molecular weight compounds, may either be more readily used by
61 microbes than existing soil C (Kayranli et al., 2010; Megonigal et al., 1999) or may prime microbial use
62 of soil C (Basiliko et al., 2012; Philippot et al., 2009; Robroek et al., 2016; Waldo et al., 2019). Root
63 exudates can also decrease CH₄ oxidation by stimulating use of O₂ by other aerobic microbes (Lenzowski
64 et al., 2018; Mueller et al., 2016). Consequently, wetland CH₄ emissions are strongly linked to a wide
65 variety of plant traits that govern the supply of reductive (organic carbon) and oxidative (O₂) substrates to
66 soils (Moor et al., 2017; Mueller et al., in press).

67 Although it is understood that wetland plants are a primary control on CH₄ emissions and that much
68 of their influence is mediated through conditions in the rhizosphere (Waldo et al., 2019), there are
69 surprisingly few data, especially from coastal wetlands, that couple plant responses to the dynamics of
70 electron donors (organic C), electron acceptors (O₂, SO₄), and the rates of competing (sulfate reduction vs
71 methanogenesis) or opposing (CH₄ production vs CH₄ oxidation) microbial processes. The general lack of
72 process data on wetland CH₄ cycling makes it difficult to forecast ecosystem responses to climate change.
73 For example, the well-documented observation that warming increases wetland methane emissions can be
74 either amplified or dampened depending on changes in plant activity (e.g. primary production) or plant
75 traits (e.g. community composition) (Mueller et al., in press). Vegetation composition has been shown to
76 be a stronger control on CH₄ emissions than ~1 °C of warming in northern peatlands (Ward et al., 2013)
77 and Chen et al. (2017) proposed that warming effects on plant functional types can drive C flux responses



78 that cannot otherwise be explained by abiotic conditions. In freshwater marshes, plant species and growth
79 trends have also been linked to seasonal shifts in pools of dissolved CH₄ and DIC (Ding et al., 2005;
80 Stanley & Ward, 2010) and methanogenesis dynamics (Sorrell et al., 1997).

81 Tidal wetlands are particularly good model systems for determining the mechanisms by which
82 warming alters CH₄ emissions. Not only will the CH₄ cycle respond to the direct effects of warming, but
83 the temperature effects on the outcome of competition for electron acceptors is relatively easily observed
84 because of the abundance of SO₄. Thermodynamic theory in which terminal electron acceptors (TEAs)
85 are used in order of decreasing thermodynamic yield is commonly interpreted to mean that a system will
86 support only one form of anaerobic respiration at time, with methanogenesis occurring only when pools
87 of more energetically favorable TEAs have been depleted. However, in real systems with spatial and
88 temporal variability in the supply of electron donor substrates and TEAs, all forms of anaerobic
89 metabolism occur simultaneously (Meronigal et al. 2004, Bridgham et al., 2013). Much of this spatial and
90 temporal variation arises from the distribution and activity of roots and rhizomes as mediated by the
91 rhizosphere (Neubauer et al., 2008). Global change factors such as warming will further affect the spatial
92 distribution of key metabolic substrates. In addition, the relatively limited species diversity in saline tidal
93 wetlands allows species-level effects on CH₄ cycling to be delineated more easily than in diverse
94 freshwater wetlands.

95 Methane flux measurements are a metric of broader shifts in redox potential and biogeochemical
96 cycling, as they are sensitive to virtually all processes that regulate availability of electron donors and
97 electron acceptors. Emissions are commonly predicted to increase with future climate warming, including
98 from coastal wetlands (Al-Haj & Fulweiler, 2020), but there is minimal prior understanding of the
99 underlying mechanisms, which was the focus of this study. Our objectives were to explore the
100 mechanisms that drive enhanced CH₄ emissions under warming. To accomplish this, we measured
101 monthly CH₄ emissions from 2016 through 2019 and coupled these flux measurements with analysis of
102 porewater biogeochemistry and vegetation biomass and composition.

103



104 2. Materials and Methods

105 2.1 Site Description and Experimental Design

106 The Salt Marsh Accretion Response to Temperature eXperiment (SMARTX) was established in the
107 Smithsonian’s Global Change Research Wetland (GCRew) in 2016. GCRew is part of Kirkpatrick
108 Marsh, a microtidal, brackish high marsh on the western shore of the Chesapeake Bay, USA (38°53’ N,
109 76°33’ W). Soils are organic (>80 % organic matter) to a depth of 5 m, which is typical of high marshes
110 in the Chesapeake Bay. The marsh is typically saturated to within 5-15 cm of the soil surface, but
111 inundation frequency varies across the site, from 10-20 % of high tides in high elevation areas to 30-60 %
112 of tides in low elevation areas.

113 SMARTX consists of six replicate transects, three located in each of the two dominant annual plant
114 communities (Fig. S1). In the C₃-dominated community (herein the ‘C₃ community’) the C₃ sedge
115 *Schoenoplectus americanus* (herein *Schoenoplectus*) composes more than 90 % of the aboveground
116 biomass (Table 1). In the C₄-dominated community (herein the ‘C₄ community’), 75 % of the
117 aboveground biomass was initially composed of two C₄ grasses (*Spartina patens* and *Distichlis spicata*,
118 herein *Spartina* and *Distichlis*, respectively). However, by 2019, *Spartina* and *Distichlis* declined to 56 %
119 of the aboveground biomass (Table 1).

Table 1. Relative contribution to total aboveground biomass from C₃ sedges (*Schoenoplectus americanus*) and C₄ grasses (*Spartina patens* and *Distichlis spicata*) in each plant community. Values are means and SE (n = 12).

Year	C ₃ community		C ₄ community	
	% C ₃	% C ₄	% C ₃	% C ₄
2016	93 (3)	8 (3)	8 (2)	76 (6)
2017	91 (3)	9 (3)	10 (3)	64 (4)
2018	95 (1)	5 (1)	15 (4)	65 (7)
2019	93 (2)	4 (1)	23 (5)	56 (6)

120 Each transect is an active warming gradient consisting of unheated ambient plots and plots that
121 are heated to 1.7 °C, 3.4 °C, and 5.1 °C above ambient. All plots are 2 x 2 meters with a 20 cm-wide
122 buffer around the perimeter. Aboveground plant-surface temperature is elevated via infrared heaters and
123 soil temperature is elevated via vertical resistance cables (Rich et al., 2015). Soils are heated to a depth of
124 1.5 m, which is the depth most vulnerable to climate or human disturbance (Pendleton et al., 2012).



125 Aboveground and belowground temperature variation are assessed via thermocouples embedded in
126 acrylic plates at plant canopy level and inserted into the soil, respectively, and the temperature gradient is
127 maintained by integrated microprocessor-based feedback control (Rich et al., 2015). Noyce et al. (2019)
128 provides additional details of the heating system. Warming began on 1 Jun 2016 and has continued year-
129 round.

130 2.2 Methane flux measurements

131 Methane emissions were measured monthly year-round from May 2016 to Dec 2019 using a static
132 chamber system. One permanent 160 cm² aluminum base was inserted 10 cm into the soil in each plot in
133 Apr 2016. On each measurement date, clear chambers (40 x 40 x 40 cm) were gently placed on top of
134 each base and secured with compression clips. Chambers consisted of an aluminum frame with
135 transparent sides made of polychlorotrifluoroethylene film (Honeywell International) and closed-cell
136 foam on the base. Depending on the height of the vegetation at the time of measurement, chambers were
137 stacked up to four high (total height of 40 to 160 cm) (Fig. S2). The advantage of this stacking method is
138 that it uses the minimal chamber volume necessary, while also allowing for plant growth. After
139 placement, the chambers were left open for at least 10 minutes, to minimize disturbance effects and allow
140 air inside the chamber to return to ambient conditions. During data collection, chambers were covered
141 with a transparent polycarbonate top equipped with sampling tubes, a fan to circulate air inside the
142 chambers, a PAR sensor, and thermocouples. The sealed chamber was covered with a foil shroud to block
143 out all light and to minimize changes in temperature and relative humidity during the measurement
144 period. An UltraPortable Greenhouse Gas Analyzer (Los Gatos Research, CA) was used to measure
145 headspace CH₄ concentrations for 5 min. Plots were accessed from permanent boardwalks elevated 15 cm
146 above the soil surface to avoid compressing the surrounding peat and altering CH₄ emissions. Fluxes were
147 calculated as the slope of the linear regression of CH₄ concentration over time. The 40 fluxes where $p >$
148 0.05 were assigned a value of ½ the limit of detection of the system (Wassmann et al., 2018; Table S1).
149 This was 1 % of fluxes during the growing season and 4.5 % of fluxes over the remaining months. For
150 2017-2019, monthly measurements were scaled to annual estimates by regressing CH₄ emissions against



151 daily mean soil temperature and day of year (as a proxy for phenological status). Annual estimates were
152 not calculated for 2016 because flux measurements did not start until May.

153 2.3 Porewater sampling and analysis

154 Porewater samples were collected in May, Jul, and Sep of each year using stainless steel ‘sippers’
155 permanently installed in each plot. Each sipper consisted of a length of stainless-steel tubing, crimped and
156 sealed at the end, with several slits (approximate width 0.8 mm) cut in the bottom 2 cm. The aboveground
157 portion of each sipper was connected to Tygon Masterflex® tubing capped with a 2-way stopcock. In
158 May 2016, duplicate clusters of sippers were installed in each of the 30 plots at 20, 40, 80, and 120 cm
159 below the soil surface. An additional set of 10 cm-deep sippers was installed in 2017. In this study we
160 defined samples from 10-20 cm as “rooting zone” samples and samples from 40-120 cm as “deep peat”
161 samples. On sampling dates, porewater sitting in the sippers was drawn up and discarded, after which 60
162 mL of porewater from each depth (30 mL from each sipper) was withdrawn and stored in syringes
163 equipped with 3-way stopcocks. A 10 mL-aliquot of each sample was filtered through a pre-leached 0.45
164 µm syringe-mounted filter, preserved with 5 % zinc acetate and sodium hydroxide, and frozen for future
165 SO₄ and Cl analysis. Dissolved CH₄ was extracted from 15 mL of porewater in the syringe by drawing 15
166 mL of ambient air and shaking vigorously for 2 min to allow the dissolved CH₄ to equilibrate with the
167 headspace. Headspace subsamples were then immediately analyzed on a Shimadzu GC-14A gas
168 chromatograph equipped with a flame ionization detector. The remaining porewater was used to measure
169 pH, H₂S, and NH₄; those data are not reported here.

170 SO₄ and Cl were measured on a Dionex ICS-2000 ion chromatography system (2016-2018) or a
171 Dionex Integrion (2019). On the Dionex ICS-2000 samples were separated using an AA11 column with
172 30 mM of KOH as eluent; on the Dionex Integrion samples were separated using an AA11-4µm-fast
173 column with 35 mM KOH. Sulfate depletion (Sulfate_{Dep}) was calculated based on measured porewater
174 concentrations of SO₄ (SO_{4pw}) and Cl (Cl_{pw}) and the constant molar ratio of Cl to SO₄ in surface seawater
175 (R_{sw} = 19.33; Bianchi 2006) using the following equation: Sulfate_{Dep} = Cl_{pw} / R_{sw} - SO_{4pw}. Based only on
176 seawater inputs, the ratio of Cl to SO₄ would remain constant, but under anaerobic conditions SO₄ can be



177 reduced by sulfate reducing bacteria, altering this ratio. As a result, SO₄ depletion can be used as a proxy
178 for SO₄ reduction rates.

179 2.4 Plant biomass measurements

180 Measurements of *Schoenoplectus*, *Spartina*, and *Distichlis* biomass were conducted during peak
181 biomass of each year (29 Jul – 2 Aug) as described by Noyce et al. (2019). *Schoenoplectus* biomass was
182 estimated using non-destructive allometric techniques (Lu et al., 2016) in 900-cm² quadrats, and *Spartina*
183 and *Distichlis* biomass were estimated through destructive harvest of 25-cm² subplots.

184 2.5 Data analysis

185 Statistics were conducted in R (version 3.6.3). ANOVA tests were used to compared means between
186 warming treatments and plant communities, with Tukey's HSD test for *post hoc* analyses. The 'growing
187 season' was defined as May through Sep, based on *Schoenoplectus* growth trends (see Fig. S3). Due to
188 the non-normal distribution of the CH₄ flux (Fig. S4) and porewater data, values were log transformed
189 prior to calculating analyses.

190

191 **3. Results**

192 3.1 Environmental conditions and experiment performance

193 The growing season of 2016 was the hottest of the four years, with growing season temperatures
194 averaging >1 °C above the other three years (Table 2). While 2017 through 2019 had similar summer
195 temperatures, they had very different precipitation regimes; 2018 was much wetter on average and 2019
196 was slightly drier (Table 2). During all years, temperatures in the experimental plots were successfully
197 shifted by the target differentials of +1.7, +3.4, and +5.1 °C above the ambient plots (Fig. 1; Noyce et al.,
198 2019).

Table 2. Growing season (May-Sep) temperature and precipitation. Temperature data are means (SE) of daily averages from ambient plots and precipitation is total from May through September.

Year	Mean aboveground temperature (°C)	Mean soil temperature (°C)	Total precipitation (cm)
2016	24.7 (0.3)	22.4 (0.2)	51.0
2017	22.0 (0.3)	20.7 (0.2)	51.1
2018	23.7 (0.3)	20.8 (0.2)	86.4
2019	23.6 (0.3)	20.9 (0.2)	43.7



199 3.2 Methane fluxes

200 Methane emissions increased with soil temperature ($R^2 = 0.41$, $p < 0.001$) (Fig. 1). Emissions from
201 all treatments had strong seasonal trends; fluxes were highest in the C_3 community in Jun through Aug
202 and peak fluxes in the C_4 community were shifted about a month later to Jul through Sep (Fig. S4).
203 Whole-ecosystem warming increased CH_4 emissions throughout the growing season ($F_{3,439} = 3.7$, $p =$
204 0.012 ; Fig. 2). Across all four years, $5.1\text{ }^\circ\text{C}$ of warming more than doubled growing season emissions,
205 from 624 to $1413\text{ }\mu\text{mol CH}_4\text{ m}^{-2}\text{ d}^{-1}$ ($p_{\text{adj}} = 0.01$; Fig. 2).

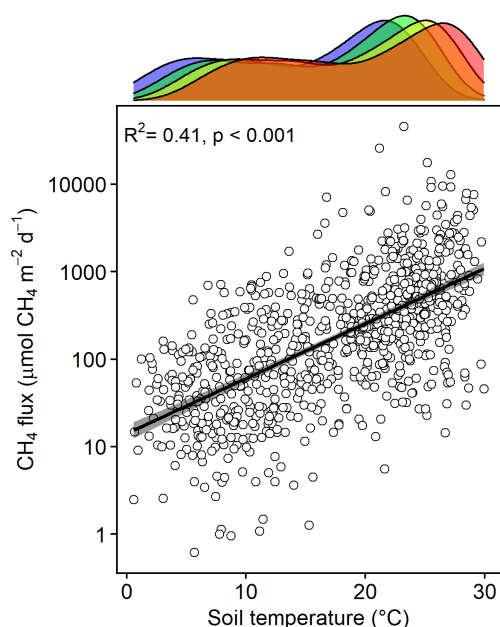


Figure 1. CH_4 emissions from each plot versus the soil temperature at the time of measurement. Density plot shows the range of soil temperatures in each treatment.

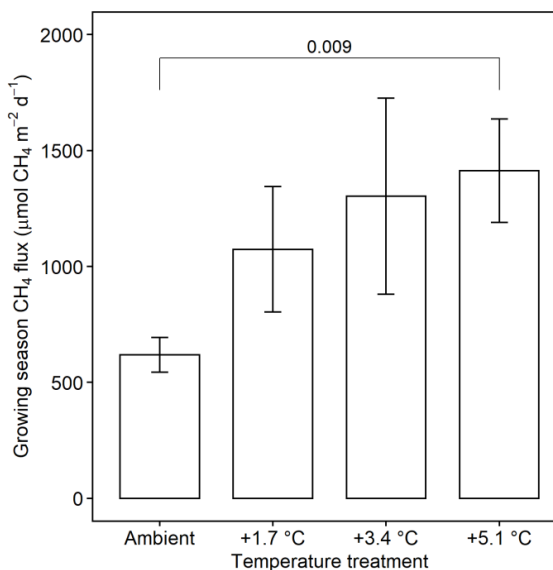


Figure 2. Comparison of CH_4 emissions from each warming treatment during the growing season (May-Sep). Means include both the C_3 and C_4 community and all years of measurement. Error bars indicate SE. Horizontal bars indicate means that are significantly different and the corresponding p_{adj} .

206 Mean CH_4 emissions were higher from the C_4 community than from the C_3 community both during
207 the growing season ($F_{1,70} = 22.0$, $p < 0.001$; Fig. 3a) and on an annual basis ($F_{1,70} = 10.2$, $p = 0.002$; Fig.
208 3b). Mean annual CH_4 emissions ranged from $58\text{ mmol CH}_4\text{ m}^{-2}\text{ yr}^{-1}$ (ambient) to $343\text{ mmol CH}_4\text{ m}^{-2}\text{ yr}^{-1}$
209 ($+5.1\text{ }^\circ\text{C}$) in the C_3 community and from $55\text{ mmol CH}_4\text{ m}^{-2}\text{ yr}^{-1}$ (ambient) to $879\text{ mmol CH}_4\text{ m}^{-2}\text{ yr}^{-1}$ ($+5.1$



210 °C) in the C₄ community (Table S2). Under ambient conditions, growing season CH₄ fluxes were almost
211 twice as large from C₄ plots, whereas under low warming (1.7-3.4 °C) this difference increased to more
212 than three times as large (Fig. 3a). From 2017-2019, CH₄ emissions were positively related to *Spartina*
213 and *Distichlis* aboveground biomass across all warming treatments and negatively related to
214 *Schoenoplectus* biomass (Fig. 4a,b). In 2016, however, the direction of those relationships in both plant
215 communities were the exact opposite, with *Spartina* and *Distichlis* biomass negatively related, and
216 *Schoenoplectus* biomass positively related, to CH₄ emissions (Fig. 4a,b).

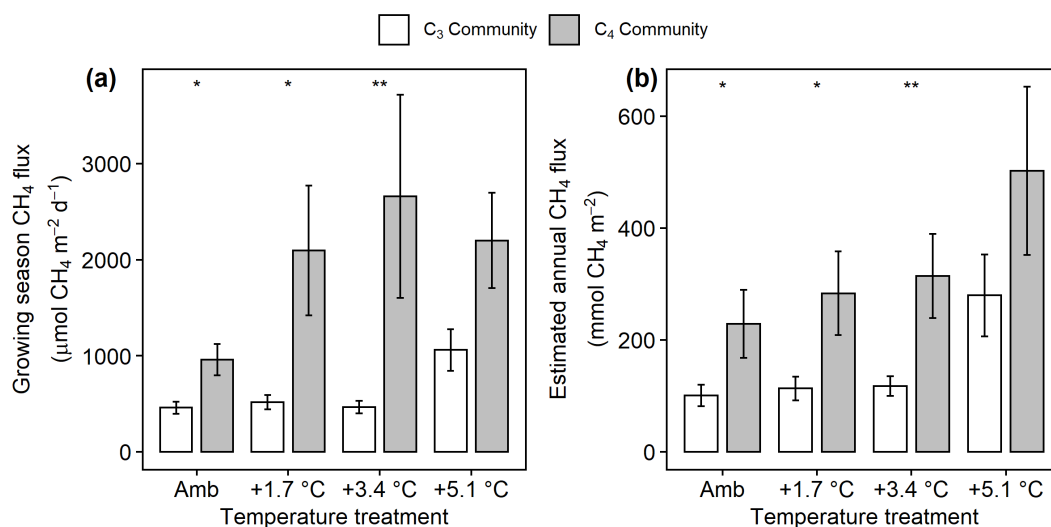


Figure 3. Comparison of CH₄ emissions from the C₃ community dominated by *Schoenoplectus* (open bars) and the C₄ community dominated by *Spartina* and *Distichlis* (grey bars). (a) During the growing season (May-Sep) and (b) scaled to a year. Means are averaged across all sampling dates for 2017 – 2019. Error bars indicate SE. Asterisks indicate significant differences between C₃ and C₄ means at a given temperature (* p_{adj} < 0.05, ** p_{adj} < 0.01).

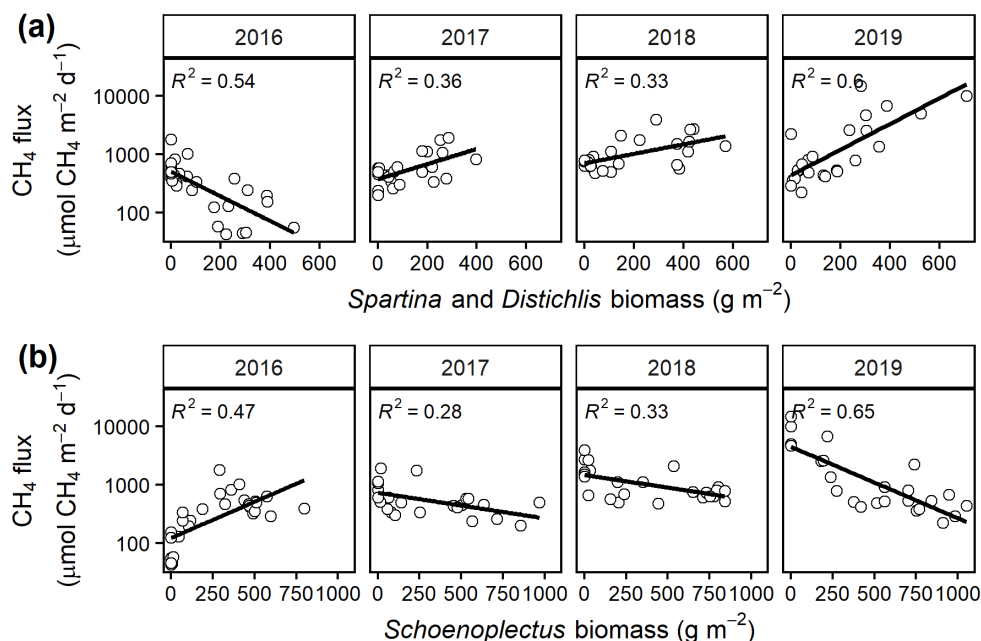


Figure 4. Mean growing season (May-Sep) CH₄ emissions from each plot versus the biomass of (a) C₃ (*Schoenoplectus*) and (b) C₄ (*Spartina* and *Distichlis*) plants. All regressions are significant at $p = 0.05$.

217 3.3 Porewater chemistry

218 Under ambient conditions, porewater collected from the C₄ community had lower salinity ($F_{1,315} =$
 219 15.5, $p < 0.001$), more dissolved CH₄ ($F_{1,315} = 45.0$, $p < 0.001$; Fig. 5a,b), and less SO₄ ($F_{1,315} = 61.5$, $p <$
 220 0.001; Fig 6a) than the C₃ community. In the C₃ community, warming increased dissolved CH₄ in both
 221 the rooting zone porewater (i.e. 10-20 cm) ($F_{3,225} = 5.45$, $p = 0.001$; Fig. 5a) and in the deep peat (40-120
 222 cm) ($F_{3,368} = 13.6$, $p < 0.001$; Fig. 5b). Dissolved CH₄ concentrations were relatively similar in the
 223 ambient, +1.7 °C, and +3.4 °C treatments, but more than doubled with +5.1 °C of warming in both the
 224 rooting zone (59 to 125 μmol CH₄ L⁻¹, $p_{\text{adj}} = 0.001$) and the deeper porewater (43 to 1254 μmol CH₄ L⁻¹,
 225 $p_{\text{adj}} < 0.001$). In the C₄ community there was minimal effect of warming treatment on porewater in the
 226 rooting zone ($F_{3,230} = 5.45$, $p = 0.67$; Fig. 5a), but all levels of warming decreased dissolved CH₄ below 40
 227 cm ($F_{3,379} = 39.3$, $p < 0.001$), with concentrations in the +3.4 and +5.1 plots less than a third of the
 228 concentrations in the ambient plots (155 vs 56 and 40 μmol CH₄ L⁻¹, $p_{\text{adj}} < 0.001$; Fig. 5b).

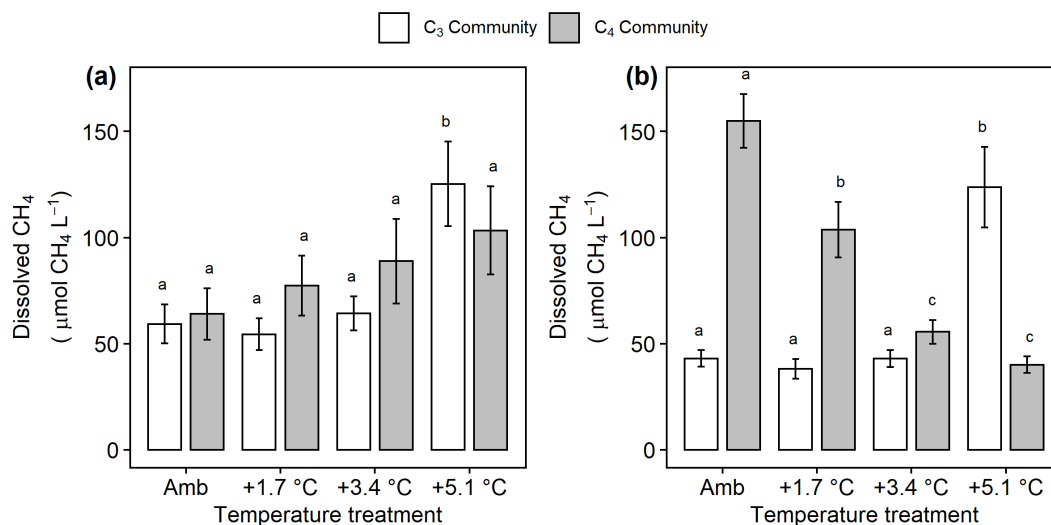


Figure 5. Comparison of dissolved CH₄ from the C₃ community dominated by *Schoenoplectus* (open bars) and the C₄ community dominated by *Spartina* and *Distichlis* (grey bars). (a) In the dominant rooting zone (10-20 cm) and (b) below the rooting zone (40-120 cm). Means are averaged across all sampling dates for 2016 – 2019. Error bars indicate SE. Letters indicate temperature treatments that are significant different from each other ($p_{adj} < 0.05$) within the same plant community.

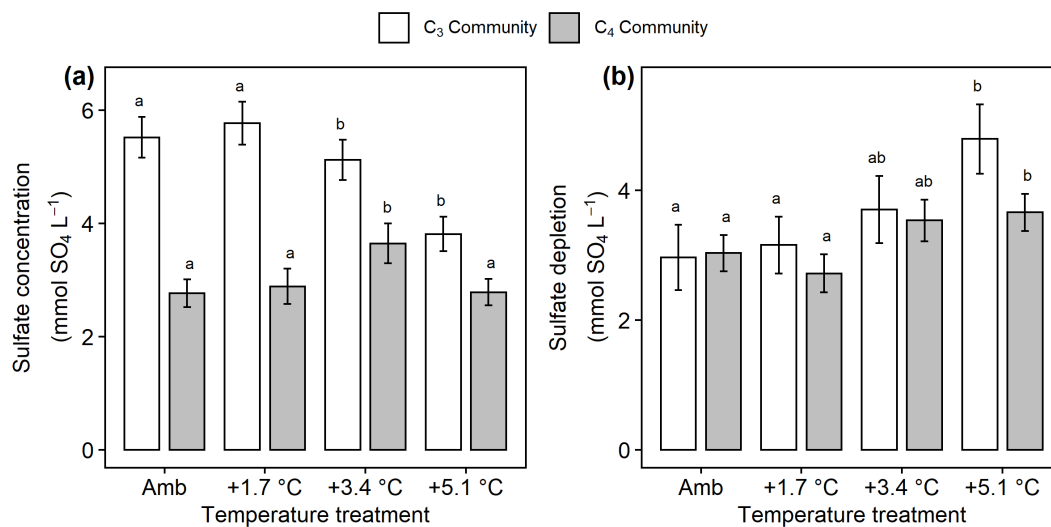


Figure 6. Comparison of sulfate concentrations and estimated sulfate depletion from the C₃ community dominated by *Schoenoplectus* (open bars) and the C₄ community dominated by *Spartina* and *Distichlis* (grey bars). (a) Sulfate in the entire soil profile and (b) sulfate depletion in the rooting zone. Means are averaged across all sampling dates for 2016 – 2019. Error bars indicate SE. Letters indicate temperature treatments that are significant different from each other ($p_{adj} < 0.05$) within the same plant community.

229 In the C₃ community, warming of +3.4 and +5.1 °C reduced SO₄ concentrations ($F_{3,597} = 11.7$, $p <$



230 0.001), but warming effects on SO_4 cycling in the C_4 community were more mixed with +3.4 °C
231 increasing SO_4 ($p_{\text{adj}} = 0.013$) but no other treatments having large effects (Fig. 6a). In all plots, the
232 measured concentrations of rooting zone SO_4 were lower than expected based on salinity (Fig. 6b),
233 indicating that SO_4 reduction occurred. In both plant communities, the +5.1 °C treatments increased this
234 SO_4 depletion effect compared to ambient (C_3 : $F_{3,349} = 3.96$, $p = 0.008$; C_3 : $F_{3,358} = 3.04$, $p = 0.029$) (Fig.
235 6b). In both plant communities, dissolved CH_4 was highest when SO_4 concentrations were below 5 mmol
236 $\text{SO}_4 \text{ L}^{-1}$ (Fig. S5).

237

238 **4. Discussion**

239 Soil temperature (both seasonal and experimental) and plant traits were both strong drivers of CH_4
240 emissions from this site. This follows prior field, mesocosm, and incubation studies across a variety of
241 wetlands, in which temperature has been shown to be a strong predictor of CH_4 emissions (e.g. Al-Haj
242 and Fulweiler, 2020; van Bodegom and Stams, 1999; Christensen et al., 2003; Dise et al., 1993; Fey and
243 Conrad, 2000; Liu et al., 2019; Ward et al., 2013; Yang et al., 2019; Yvon-Durocher et al., 2014) and in
244 which plant functional type has an interacting effect (Chen et al., 2017; Duval & Radu, 2018; L. Liu et al.,
245 2019; Mueller et al., in press; Ward et al., 2013). Methane emissions are a function of the balance
246 between methanogenesis, CH_4 oxidation, and CH_4 transport, so explaining these results requires some
247 combination of stimulation of methanogenesis, reduction of CH_4 oxidation, or increase in CH_4 transport.

248 Prior data from brackish wetlands are limited, but incubation studies on freshwater wetland soils
249 typically show large increases in CH_4 fluxes with warming (Duval & Radu, 2018; Hopple et al., 2020;
250 Inglett et al., 2012; Sihi et al., 2017; van Bodegom & Stams, 1999; Wilson et al., 2016), indicating that
251 warming alters belowground processes. Though there is some evidence that rhizosphere temperature
252 alters CH_4 transport through rice aerenchyma (Hosono & Nouchi, 1997), any transport-driven effects in
253 this ecosystem would be transient unless there was a simultaneous increase in net CH_4 production (i.e. an
254 increase in methanogenesis that was not completely offset by methanotrophy). Instead, we observed a
255 sustained increase in CH_4 emissions, suggesting large shifts in anaerobic metabolism, especially with +5.1



256 °C of warming. We propose four potential and non-exclusive mechanisms to explain the temperature-
257 driven increase in CH₄ emissions: (1) shifted ratios of CH₄ production to oxidation, (2) increased substrate
258 availability, (3) reduced competition with sulfate reducers, and (4) indirect plant trait effects (Fig. 7).

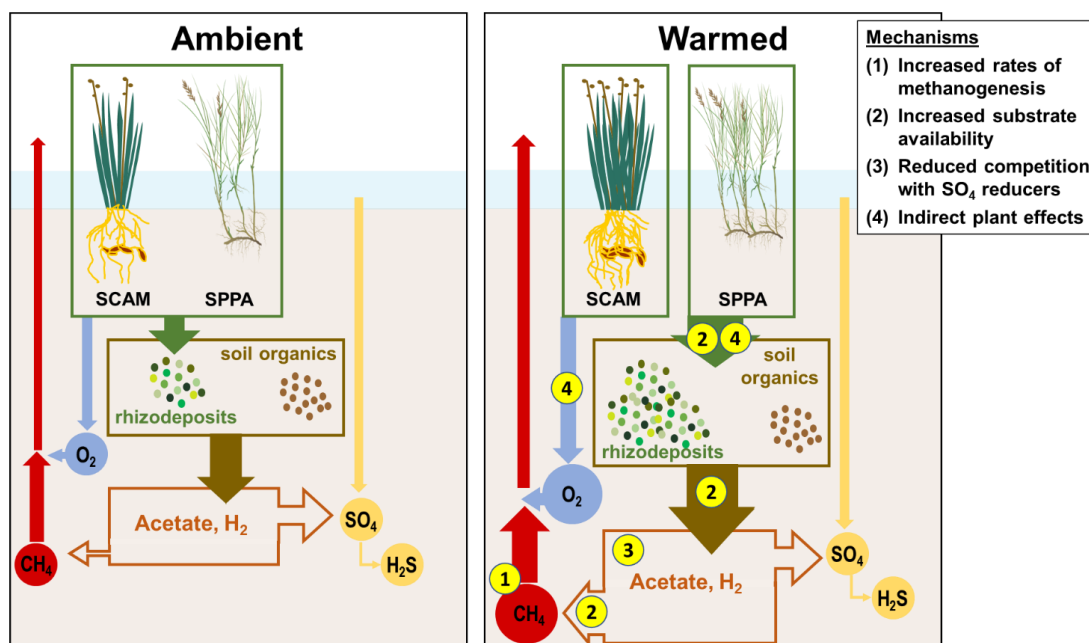


Figure 7. Schematic of mechanisms driving enhanced CH₄ emissions in response to warming. SCAM = *Schoenoplectus americanus*. SPPA = *Spartina patens*. Left: Processes under ambient conditions. Plants add organic compounds to the soil, which are transformed into other low molecular weight organic compounds. This pool, and processed soil organic matter, support terminal respiration processes dominated by SO₄ reduction over CH₄ production in organic-rich brackish marsh soils. Plants also transport O₂ which supports oxidation of a fraction of the CH₄ before it can be transported out of the soil. Right: Processes under warmed conditions. 1) Rates of CH₄ production increase more than rates of CH₄ oxidation. 2) Substrate availability increases as plants add more rhizodeposits and organic matter is more rapidly fermented to low molecular weight organic compounds and H₂. 3) The pool of electron donors available to methanogens increases as SO₄ reducers become SO₄ limited. 4) The dominant plant species have different effects on these process with *S. americanus* driving a net increase in O₂ transport and *S. patens* driving a net increase in rhizodeposits.

259 4.1 Whole-ecosystem warming promotes methanogenesis over CH₄ oxidation

260 Holding the supply of substrates and transport properties of the system constant, warming is expected
261 to increase rates of CH₄ production relative to CH₄ oxidation due solely to differences in the temperature
262 dependence of each process (Megonigal et al., 2016). In wetland soils, the average Q₁₀ of methanogenesis
263 is 4.1 compared to 1.9 for aerobic CH₄ oxidation (Segers, 1998), which means that a system starting with



264 a given initial ratio between the two processes will become increasingly dominated by methanogenesis as
265 soils warm. A corollary to this expected pattern is that the ratio of the two processes should be constant if
266 the Q_{10} responses are similar, an outcome that was supported with *in situ* measurements of the two
267 processes in a tidal freshwater forested wetland (Meronigal & Schlesinger, 2002). We did not quantify
268 the temperature dependence of CH_4 production and oxidation in the present study, but based on the
269 literature (Segers, 1998) it is likely that methanogenic activity increased more than aerobic
270 methanotrophic activity in direct response to warming (Fig. 7, mechanism 1). Evidence for this is that
271 rhizosphere pools of porewater CH_4 were highest in the warmest treatment (Fig. 5a); because this
272 occurred despite either no change or an increase in aboveground biomass (Noyce et al., 2019) which
273 would by itself have lowered porewater CH_4 due to venting (plant transport), it indicates that CH_4
274 production increased relative to the sum of aerobic and anaerobic methane oxidation.

275 4.2 Whole-ecosystem warming increases substrate availability for methanogens

276 Methanogenesis can be the terminal step of anaerobic decomposition, but a consortium of microbes is
277 required to break down soil organic matter to electron donor substrates that methanogens can metabolize.
278 The final step in any decomposition pathway involves the flow of electrons from organic matter (electron
279 donors) to a TEA. Under anaerobic conditions, this is accomplished by microbes that tend to specialize in
280 one TEA and compete for organic C as an electron donor (Meronigal et al., 2004). Consequently, the
281 supply of both electron donors and TEAs regulate the multi-step process of anaerobic decomposition and
282 thus ultimately control CH_4 emissions. Methanogenic activity is typically limited by the supply of
283 electron donors, including low molecular weight organic compounds (e.g. acetate, Neubauer & Craft,
284 2009) and H_2 , a product of organic matter fermentation. We propose that whole-ecosystem warming
285 increases the availability of previously limited C substrates through two pathways (Fig. 7, mechanism 2).

286 First, warming may directly influence C availability through biochemical kinetics. Even if organic
287 inputs remained constant, warming likely accelerates fermentation of soil organic matter, presumably
288 increasing substrate availability for methanogens. Second, the warmed plots had longer growing seasons



289 than the unheated controls (Noyce et al., 2019). This increases inputs of root exudates and fresh detritus,
290 accelerating all forms of heterotrophic microbial respiration by providing organic material that can be
291 broken down into acetate, H₂, and other electron donors (Philippot et al., 2009) and stimulating CH₄
292 emissions from warmed plots, particularly during the growing season as seen here. In 2017, we measured
293 GPP at the same time as CH₄ emissions and observed that CH₄ emissions were positively correlated with
294 GPP and that this effect increased with warming (Fig. S6). Prior studies have also linked CH₄ production
295 or emissions to rates of photosynthesis (Vann & Megonigal, 2003), periods of active growth (Chen et al.,
296 2017; Ward et al., 2013), and plant senescence which coincides with a pulse of labile C from plants to
297 soils (Bardgett et al., 2005).

298 4.4 Whole-ecosystem warming reduces competition with sulfate reducers

299 While acetate and other low molecular weight organic compounds are important electron donors for
300 methanogenic respiration, they are also a key substrate for other microbial groups including SO₄ reducers
301 (Megonigal et al., 2004; Ye et al., 2014). As a result, consumption of the limited acetate supply by SO₄
302 reducers should (and often does) limit methanogenic activity, such that terminal microbial respiration is
303 typically dominated by SO₄ reduction in brackish marshes (Sutton-Grier et al., 2011).

304 We did not measure rates of SO₄ reduction in this study, but can use SO₄ depletion as a proxy; more
305 SO₄ depletion indicates that more SO₄ reduction has occurred. Warming generally increased SO₄
306 depletion, especially in the plots dominated by *Schoenoplectus* (Fig. 6b). Differences in SO₄ depletion
307 between plots is not driven by SO₄ inputs because the only supply of SO₄ is the tidal flow, which is the
308 same for all plots in each community of the experiment. Instead, higher rates of SO₄ reduction are most
309 likely driven by some combination of electron donor supply and kinetics. While SO₄ reducers likely
310 benefited from the increased availability of electron donors, as described above, the kinetics of SO₄
311 reduction also respond strongly to temperature (Weston & Joye, 2005).

312 When SO₄ concentrations drop below a threshold concentration, SO₄ reduction becomes SO₄-limited,
313 rather than electron donor-limited (Megonigal et al., 2004). A review of the coastal wetland CH₄ literature



314 estimated this threshold at 4 mmol SO₄ (Poffenbarger et al., 2011), a value that is consistent with patterns
315 of porewater [CH₄] and [SO₄] at the GCRew site (Keller et al. 2009). As SO₄ and O₂ are the dominant
316 electron-accepting compounds that suppress methanogenesis in this organic soil, this drawdown then
317 releases the methanogens from substrate competition (Fig. 7, mechanism 3). Here, we show that [SO₄] is
318 typically below 4 mmol in the +5.1 plots in the C₃ community and in all plots in the C₄ community (Fig.
319 6, Fig. S5). The drawdown of SO₄ may also reduce rates of anaerobic CH₄ oxidation (Hinrichs & Boetius,
320 2003). Van Hulzen et al. (1999) proposed a multi-phase system in a warming incubation experiment,
321 observing that first methanogens are out-competed for substrates by other microbes, next CH₄ production
322 increases as the supply of inhibiting TEA decreases, and finally [TEA] decreases to the point that
323 methanogenesis is controlled only by the supply of electron donors. Warming in this study decreased time
324 required for the system to pass through the first two phases (van Hulzen et al., 1999). In our study, this
325 final phase of increased methanogenic activity occurs when SO₄ concentrations dip below 4 mmol SO₄ L⁻¹,
326 which occurs most often in the +5.1 °C plots, especially in the C₃ community. This interpretation is also
327 supported by the long-term record of porewater chemistry from an allied experiment at the site,
328 demonstrating that porewater CH₄ concentrations increase as SO₄ concentrations decrease (Keller et al.,
329 2009).

330 Methanogens may also have a competitive advantage over SO₄ reducers for electron donor
331 consumption at warmer temperatures (van Hulzen et al., 1999). Sulfate reducers and methanogens have
332 very similar K_M values for acetate, but the K_M for acetoclastic methanogenesis may decrease with
333 temperature whereas K_M values for SO₄ reducers increase with temperature (van Bodegom & Stams,
334 1999). If this is the case in our system then warming would allow methanogens to use a greater proportion
335 of the available acetate and other organic compounds.

336 4.5 Plant traits modify warming effects on CH₄ cycling

337 The three biogeochemical mechanisms we propose to explain a warming-induced increase in CH₄
338 emissions should interact strongly with plant responses to warming. Relationships between plant



339 functional groups and CH₄ emissions have been demonstrated through field studies in other wetland
340 ecosystems such as peatlands (Bubier et al., 1995; Ward et al., 2013) (Bubier et al., 1995, Ward et al.,
341 2013) and in tidal wetland mesocosms (L. Liu et al., 2019; Martin & Moseman-Valtierra, 2017; Mueller
342 et al., in press). We provide field evidence that two species with distinct plant traits -- *Schoenoplectus* and
343 *Spartina* -- have strikingly different effects on CH₄ emissions from brackish wetlands. *Spartina*-
344 dominated communities had consistently higher CH₄ emissions under both ambient and warmed
345 conditions (Fig. 3). In most years, *Schoenoplectus* biomass was negatively correlated with CH₄ emissions,
346 while *Spartina/Distichlis* biomass was positively correlated. Vegetation effects are typically strongest
347 during the growing season, when the plants are actively altering rhizosphere biogeochemistry (F.-J. W. A.
348 van der Nat & Middelburg, 1998; Ward et al., 2013), which is consistent with our observations in this
349 study.

350 As with warming effects, plant-driven shifts in CH₄ emissions are the result of differing rates of CH₄
351 production, oxidation, transport, or a combination of these processes, but sustained differences in
352 emissions cannot be attributed only to transport, as discussed previously. Instead, the stimulation of CH₄
353 emissions is likely due to changes in the plant-mediated supply of electron acceptors and electron donors.
354 In a field environment, differentiating between species-specific effects and underlying environmental
355 conditions can be difficult, but mesocosm studies that control all environmental factors have also found
356 species-specific effects on CH₄ cycling (e.g. (D. Liu et al., 2014). Plants can alter CH₄ cycling by adding
357 O₂ (electron acceptor) or C substrates (electron donors) to the rhizosphere, altering the redox state. We
358 propose that *Schoenoplectus* is a net oxidizer of the rhizosphere and that *Spartina* is a net reducer, and
359 thus their presence and productivity have opposing effects on CH₄ emissions (Fig. 7, mechanism 4).

360 4.5.1 *Schoenoplectus* oxidizes the rhizosphere, increasing CH₄ oxidation

361 Species vary in their capacity to support aerobic CH₄ oxidation (van der Nat & Middelburg, 1998)
362 and *Schoenoplectus* appears to support higher rates of aerobic CH₄ oxidation than *Spartina* (Mueller et
363 al., in press). *Scirpus lacustris* is morphologically similar to *Schoenoplectus americanus* studied here and



364 has been demonstrated to have substantial rhizospheric oxidation capacity, especially during the growing
365 season (van der Nat & Middelburg, 1998). Consequently, these plants likely exert stronger control on
366 rates of CH₄ oxidation than rates of methanogenesis (van der Nat & Middelburg, 1998). We hypothesize
367 that the relatively high capacity of *Schoenoplectus* to transport O₂ held the CH₄ emissions stimulation
368 caused by modest levels of warming (+1.7 to +3.4 °C) to rates similar to under ambient conditions (Fig.
369 3). At high warming (+5.1 °C), however, *Schoenoplectus* community CH₄ emissions drastically increase
370 (Fig. 3). We suggest that this is due to the combined effects of the three mechanisms discussed
371 previously, namely the differences in the Q₁₀-values of CH₄ production and CH₄ oxidation, the increased
372 supply of organic substrate through plant productivity, and the decrease in competition for electron
373 donors due to SO₄ depletion. Collectively, when the ecosystem is warmed above current ambient
374 conditions by 5 °C or more, enhanced stimulation of CH₄ production starts to offset some of the
375 *Schoenoplectus* oxidation effect. This also offers an explanation for the positive correlation between
376 *Schoenoplectus* biomass and CH₄ emissions observed in 2016 as that was the hottest of the four years in
377 this study.

378 4.5.2 *Spartina* reduces the rhizosphere, increasing CH₄ production

379 The variability in quality and quantity of root exudates between plant functional types is well known
380 to affect microbial community composition and activity (Deyn et al., 2008). Methanogenesis responses to
381 warming in incubation studies are related to the lignin and cellulose content of the peat, which in turn
382 depends on the plant functional type from which the peat developed (Duval & Radu, 2018). Although
383 warming is likely increasing substrate availability across the whole experiment, the production rate of
384 labile, low molecular weight C substrates through fermentation does not increase as rapidly above 25 °C
385 (Scott C Neubauer & Craft, 2009; Weston & Joye, 2005). Microbes may also preferentially use root
386 exudates as their C sources (Delarue et al., 2014) and consequently warming effects on CH₄ production
387 should be strongest in a system where the plants are directly releasing key C substrates. We propose this
388 explains the patterns that we observed in the C₄ community. Multiple years of porewater chemistry at this



389 site show that *Spartina*-dominated communities have higher DOC and dissolved CH₄ than adjacent
390 *Schoenoplectus* communities (Keller et al., 2009; Marsh et al., 2005). Though we did not directly measure
391 root exudation, porewater DOC is partially derived from root exudation and has been used as a proxy to
392 understand the responses of root exudates to global change factors (Dieleman et al., 2016; Fenner et al.,
393 2007; Jones et al., 2009).

394 In most years, *Spartina* biomass was positively correlated with CH₄ emissions, supporting our
395 hypothesis that *Spartina* favors net CH₄ production. However, in 2016 *Spartina* biomass and CH₄
396 emissions were negatively correlated. Prior work at this site has indicated that *Spartina/Distichlis* biomass
397 is more negatively affected by hot and dry growing conditions than *Schoenoplectus* (Noyce et al., 2019)
398 due in part because the *Spartina/Distichlis* (C₄) communities are less frequently inundated. The 2016
399 growing season was substantially warmer than average (Table 2) and the heating treatments were
400 initialized on 1 Jun of that year, after the annual plants had already established and may have developed
401 adaptations to ambient, rather than elevated, temperature conditions. The combination of these two effects
402 likely led to heat stress, reducing the root exudates supplied to the rhizosphere microbial community
403 (Heckathorn et al., 2013) and thus minimizing the *Spartina* stimulation effect.

404 4.6 Comparisons with prior data

405 Methane emissions have been measured at the GCRew site previously, but this study represents the most
406 comprehensive dataset collected to date, and is thus particularly useful for advancing the process-based
407 understanding needed to improve prognostic models. Overall, our flux estimates are lower than those
408 reported previously. The earliest CH₄ fluxes were measured in a single month (July) in *Schoenoplectus*-
409 dominated plots and reported to be 331 to 6883 μmol m⁻² d⁻¹ (Dacey et al., 1994), much higher than our
410 range of 359 to 1651 μmol m⁻² d⁻¹ for ambient temperature *Schoenoplectus* plots in July. Similarly, Marsh
411 et al. (2005) reported mean growing season (May-Oct) CH₄ emissions from this site of 846 ± 111 μmol
412 CH₄ m⁻² d⁻¹, whereas we measured 656 ± 79 μmol CH₄ m⁻² d⁻¹ over the same months. Finally, Pastore et
413 al. (2017) estimated average annual fluxes in their *Schoenoplectus*-dominated ambient CO₂ plots as 3.1 ±
414 1.7 g CH₄ m⁻² yr⁻¹, compared to our estimates of 1.6 ± 0.3 g CH₄ m⁻² yr⁻¹ for *Schoenoplectus* plots. The



415 different estimates by these studies may be partly due to interannual variability as demonstrated in our
416 data where 2018 had substantially higher fluxes than any of the surrounding years (Table S2).

417 The annual estimates reported here for ambient temperature plots trended lower than published
418 mean CH₄ emissions for mesohaline tidal marshes. Our plots ranged from 0.7 to 9.3 g CH₄ m⁻² yr⁻¹ (mean
419 = 9.3), compared to the range of 3.3 to 16.4 g CH₄ m⁻² yr⁻¹ (mean = 16.4) reported by Poffenbarger et al.
420 (2011). This difference may be explained by the fact that there was significant within-class variation in
421 the oligohaline and mesohaline salinity classes that was unexplained and their assessment was based on
422 too few data points to fully capture the variation that is expected to exist in the mesohaline class. Indeed,
423 subsequent studies have documented fluxes well below 3 g CH₄ m⁻² yr⁻¹ (Krauss & Whitbeck, 2012), and
424 even negative fluxes (Al-Haj & Fulweiler, 2020). We hypothesize that the low fluxes measured at our site
425 reflect *Schoenoplectus americanus* traits that favor CH₄ oxidation more than CH₄ production, and that the
426 high end of our range was limited by the high soil elevation (i.e. deep water table) of areas dominated by
427 *Spartina patens*, off-setting the influence of *S. patens* traits that favor CH₄ production.

428 4.7 Implications for tidal wetland carbon cycling

429 Warming accelerates rates of CH₄ emissions from brackish marshes, especially during the growing
430 season. This is driven by both direct and indirect warming effects and mediated by soil biogeochemistry,
431 but the magnitude of the warming effect is also dependent on traits of the plant species that dominate the
432 plant community. Communities dominated by *Spartina patens* increase net CH₄ emissions in response to
433 smaller increments of warming than communities dominated by *Schoenoplectus americanus*. *Spartina*-
434 dominated sites may thus have a higher likelihood of shifting from a net C sink to a net C source under
435 future warming conditions, due to this increased loss of C as CH₄. However, this effect could be mitigated
436 if these high-elevation *Spartina* marshes become dominated by *Schoenoplectus* in response to predicted
437 accelerated sea-level rise (Kirwan & Guntenspergen, 2012). In addition, *Spartina* traits are plastic and
438 influenced by factors such as soil redox conditions (Kludze & DeLaune, 1994), salinity (Crozier &
439 DeLaune, 1996), and water level (Liu et al., 2019), all of which can be expected to change plant-mediated
440 effects on CH₄ biogeochemistry. Further studies are needed to thoroughly assess the range of



441 environmental conditions under which *Spartina* is a net reducer and *Schoenoplectus* is a net oxidizer as
442 proposed by the present study.

443

444 **Data availability**

445 All data is available from the corresponding author upon request.

446

447 **Author contributions**

448 GLN and JPM designed the study, GLN collected and analyzed the data, and GLN and JPM wrote the
449 paper.

450

451 **Competing interests**

452 The authors declare that they have no conflict of interest.

453

454 **Acknowledgements**

455 This manuscript is based upon work supported by the U.S. Department of Energy, Office of Science,
456 Office of Biological and Environmental Research Program (DE-SC0014413 and DE-SC0019110), the
457 National Science Foundation Long-Term Research in Environmental Biology Program (DEB-0950080,
458 DEB-1457100, and DEB-1557009), and the Smithsonian Institution. Roy Rich designed the warming
459 infrastructure and maintains it with the assistance of Gary Peresta. We also thank technicians in the SERC
460 Biogeochemistry Lab for assistance with porewater collection and analysis.

461

462 **References**

463 Al-Haj, A. N., & Fulweiler, R. W. (2020). A synthesis of methane emissions from shallow vegetated

464 coastal ecosystems. *Global Change Biology*, 26(5), 2988–3005.

465 <https://doi.org/10.1111/gcb.15046>

466 Bardgett, R. D., Bowman, W. D., Kaufmann, R., & Schmidt, S. K. (2005). A temporal approach to

467 linking aboveground and belowground ecology. *Trends in Ecology & Evolution*, 20(11), 634–

468 641. <https://doi.org/10.1016/j.tree.2005.08.005>



- 469 Basiliko, N., Stewart, H., Roulet, N. T., & Moore, T. R. (2012). Do Root Exudates Enhance Peat
470 Decomposition? *Geomicrobiology Journal*, 29(4), 374–378.
471 <https://doi.org/10.1080/01490451.2011.568272>
- 472 Bridgham, S. D., Cadillo-Quiroz, H., Keller, J. K., & Zhuang, Q. (2013). Methane emissions from
473 wetlands: Biogeochemical, microbial, and modeling perspectives from local to global scales.
474 *Global Change Biology*, 19(5), 1325–1346. <https://doi.org/10.1111/gcb.12131>
- 475 Bridgham, S. D., Megonigal, J. P., Keller, J. K., Bliss, N. B., & Trettin, C. (2006). The carbon balance of
476 North American wetlands. *Wetlands*, 26(4), 889–916. [https://doi.org/10.1672/0277-5212\(2006\)26\[889:TCBONA\]2.0.CO;2](https://doi.org/10.1672/0277-5212(2006)26[889:TCBONA]2.0.CO;2)
- 477
- 478 Bubier, J. L., Moore, T. R., Bellisario, L., Comer, N. T., & Crill, P. M. (1995). Ecological controls on
479 methane emissions from a Northern Peatland Complex in the zone of discontinuous permafrost,
480 Manitoba, Canada. *Global Biogeochemical Cycles*, 9(4), 455–470.
481 <https://doi.org/10.1029/95GB02379>
- 482 Chen, J., Luo, Y., Xia, J., Wilcox, K. R., Cao, J., Zhou, X., Jiang, L., Niu, S., Estera, K. Y., Huang, R.,
483 Wu, F., Hu, T., Liang, J., Shi, Z., Guo, J., & Wang, R.-W. (2017). Warming Effects on
484 Ecosystem Carbon Fluxes Are Modulated by Plant Functional Types. *Ecosystems*, 20(3), 515–
485 526. <https://doi.org/10.1007/s10021-016-0035-6>
- 486 Christensen, T. R., Ekberg, A., Ström, L., Mastepanov, M., Panikov, N., Öquist, M., Svensson, B. H.,
487 Nykänen, H., Martikainen, P. J., & Oskarsson, H. (2003). Factors controlling large scale
488 variations in methane emissions from wetlands. *Geophysical Research Letters*, 30(7), 1414.
489 <https://doi.org/10.1029/2002GL016848>
- 490 Crozier, C. R., & DeLaune, R. D. (1996). Methane production by soils from different Louisiana marsh
491 vegetation types. *Wetlands*, 16(2), 121–126. <https://doi.org/10.1007/BF03160685>
- 492 Dacey, J. W. H., Drake, B. G., & Klug, M. J. (1994). Stimulation of methane emission by carbon dioxide
493 enrichment of marsh vegetation. *Nature*, 370(6484), 47–49. <https://doi.org/10.1038/370047a0>
- 494 Delarue, F., Gogo, S., Buttler, A., Bragazza, L., Jassey, V. E. J., Bernard, G., & Laggoun-Défarge, F.



- 495 (2014). Indirect effects of experimental warming on dissolved organic carbon content in
496 subsurface peat. *Journal of Soils and Sediments*, 14(11), 1800–1805.
497 <https://doi.org/10.1007/s11368-014-0945-x>
- 498 Deyn, G. B. D., Cornelissen, J. H. C., & Bardgett, R. D. (2008). Plant functional traits and soil carbon
499 sequestration in contrasting biomes. *Ecology Letters*, 11(5), 516–531.
500 <https://doi.org/10.1111/j.1461-0248.2008.01164.x>
- 501 Dieleman, C. M., Lindo, Z., McLaughlin, J. W., Craig, A. E., & Branfireun, B. A. (2016). Climate change
502 effects on peatland decomposition and porewater dissolved organic carbon biogeochemistry.
503 *Biogeochemistry*, 128(3), 385–396. <https://doi.org/10.1007/s10533-016-0214-8>
- 504 Ding, W., Cai, Z., & Tsuruta, H. (2005). Plant species effects on methane emissions from freshwater
505 marshes. *Atmospheric Environment*, 39(18), 3199–3207.
506 <https://doi.org/10.1016/j.atmosenv.2005.02.022>
- 507 Dise, N. B., Gorham, E., & Verry, E. S. (1993). Environmental factors controlling methane emissions
508 from peatlands in northern Minnesota. *Journal of Geophysical Research: Atmospheres*, 98(D6),
509 10583–10594. <https://doi.org/10.1029/93JD00160>
- 510 Duval, T. P., & Radu, D. D. (2018). Effect of temperature and soil organic matter quality on greenhouse-
511 gas production from temperate poor and rich fen soils. *Ecological Engineering*, 114, 66–75.
512 <https://doi.org/10.1016/j.ecoleng.2017.05.011>
- 513 Environmental Protection Agency. (2017). *Inventory of U.S. Greenhouse Gas Emissions and Sinks: 1990-*
514 *2015*. (EPA 430-P-17-001).
- 515 Fenner, N., Freeman, C., Lock, M. A., Harmens, H., Reynolds, B., & Sparks, T. (2007). Interactions
516 between Elevated CO₂ and Warming Could Amplify DOC Exports from Peatland Catchments.
517 *Environmental Science & Technology*, 41(9), 3146–3152. <https://doi.org/10.1021/es061765v>
- 518 Fey, A., & Conrad, R. (2000). Effect of temperature on carbon and electron flow and on the archaeal
519 community in methanogenic rice field soil. *Applied and Environmental Microbiology*, 66(11),
520 4790–4797. <https://doi.org/10.1128/AEM.66.11.4790-4797.2000>



- 521 Heckathorn, S. A., Giri, A., Mishra, S., & Bista, D. (2013). Heat Stress and Roots. In *Climate Change*
522 *and Plant Abiotic Stress Tolerance* (pp. 109–136). John Wiley & Sons, Ltd.
523 <https://doi.org/10.1002/9783527675265.ch05>
- 524 Hinrichs, K.-U., & Boetius, A. (2003). The Anaerobic Oxidation of Methane: New Insights in Microbial
525 Ecology and Biogeochemistry. In G. Wefer, D. Billett, D. Hebbeln, B. B. Jørgensen, M. Schlüter,
526 & T. C. E. van Weering (Eds.), *Ocean Margin Systems* (pp. 457–477). Springer.
527 https://doi.org/10.1007/978-3-662-05127-6_28
- 528 Hopple, A. M., Wilson, R. M., Kolton, M., Zalman, C. A., Chanton, J. P., Kostka, J., Hanson, P. J.,
529 Keller, J. K., & Bridgman, S. D. (2020). Massive peatland carbon banks vulnerable to rising
530 temperatures. *Nature Communications*, *11*(1), 2373. <https://doi.org/10.1038/s41467-020-16311-8>
- 531 Hosono, T., & Nouchi, I. (1997). The dependence of methane transport in rice plants on the root zone
532 temperature. *Plant and Soil*, *191*(2), 233–240. <https://doi.org/10.1023/A:1004203208686>
- 533 Inglett, K. S., Inglett, P. W., Reddy, K. R., & Osborne, T. Z. (2012). Temperature sensitivity of
534 greenhouse gas production in wetland soils of different vegetation. *Biogeochemistry*, *108*(1–3),
535 77–90. <https://doi.org/10.1007/s10533-011-9573-3>
- 536 IPCC. (2013). *Limite Change 2013: The Physical Science Basis. Working Group I Contribution to the*
537 *Fifth Assessment Report of the Intergovernmental Panel on Climate Change.*
538 www.ipcc.ch/report/ar5/wg1/
- 539 Jones, T. G., Freeman, C., Lloyd, A., & Mills, G. (2009). Impacts of elevated atmospheric ozone on
540 peatland below-ground DOC characteristics. *Ecological Engineering*, *35*(6), 971–977.
541 <https://doi.org/10.1016/j.ecoleng.2008.08.009>
- 542 Kayranli, B., Scholz, M., Mustafa, A., & Hedmark, Å. (2010). Carbon Storage and Fluxes within
543 Freshwater Wetlands: A Critical Review. *Wetlands*, *30*(1), 111–124.
544 <https://doi.org/10.1007/s13157-009-0003-4>
- 545 Keller, J. K., Wolf, A. A., Weisenhorn, P. B., Drake, B. G., & Megonigal, J. P. (2009). Elevated CO₂
546 affects porewater chemistry in a brackish marsh. *Biogeochemistry*, *96*(1–3), 101–117.



- 547 <https://doi.org/10.1007/s10533-009-9347-3>
- 548 Kirwan, M. L., & Guntenspergen, G. R. (2012). Feedbacks between inundation, root production, and
549 shoot growth in a rapidly submerging brackish marsh. *Journal of Ecology*, *100*(3), 764–770.
550 <https://doi.org/10.1111/j.1365-2745.2012.01957.x>
- 551 Kludze, H. K., & DeLaune, R. D. (1994). Methane Emissions and Growth of *Spartina patens* in Response
552 to Soil Redox Intensity. *Soil Science Society of America Journal*, *58*(6), 1838–1845.
553 <https://doi.org/10.2136/sssaj1994.03615995005800060037x>
- 554 Krauss, K. W., & Whitbeck, J. L. (2012). Soil greenhouse gas fluxes during wetland forest retreat along
555 the Lower Savannah River, Georgia (USA). In *Wetlands* (Vol. 32, Issue 1, p. 7381).
556 <https://doi.org/10.1007/s13157-011-0246-8>
- 557 Lenzewski, N., Mueller, P., Meier, R. J., Liebsch, G., Jensen, K., & Koop-Jakobsen, K. (2018). Dynamics
558 of oxygen and carbon dioxide in rhizospheres of *Lobelia dortmanna* – a planar optode study of
559 belowground gas exchange between plants and sediment. *New Phytologist*, n/a-n/a.
560 <https://doi.org/10.1111/nph.14973>
- 561 Liu, D., Ding, W., Yuan, J., Xiang, J., & Lin, Y. (2014). Substrate and/or substrate-driven changes in the
562 abundance of methanogenic archaea cause seasonal variation of methane production potential in
563 species-specific freshwater wetlands. *Applied Microbiology and Biotechnology*, *98*(10), 4711–
564 4721. <https://doi.org/10.1007/s00253-014-5571-4>
- 565 Liu, L., Wang, D., Chen, S., Yu, Z., Xu, Y., Li, Y., Ge, Z., & Chen, Z. (2019). Methane Emissions from
566 Estuarine Coastal Wetlands: Implications for Global Change Effect. *Soil Science Society of
567 America Journal*, *83*(5), 1368–1377. <https://doi.org/10.2136/sssaj2018.12.0472>
- 568 Lu, M., Caplan, J. S., Bakker, J. D., Langley, J. A., Mozdzer, T. J., Drake, B. G., & Megonigal, J. P.
569 (2016). Allometry data and equations for coastal marsh plants. *Ecology*, *97*(12), 3554–3554.
570 <https://doi.org/10.1002/ecy.1600>
- 571 Marsh, A. S., Rasse, D. P., Drake, B. G., & Patrick Megonigal, J. (2005). Effect of elevated CO₂ on
572 carbon pools and fluxes in a brackish marsh. *Estuaries*, *28*(5), 694–704.



- 573 <https://doi.org/10.1007/BF02732908>
- 574 Martin, R. M., & Moseman-Valtierra, S. (2017). Different short-term responses of greenhouse gas fluxes
575 from salt marsh mesocosms to simulated global change drivers. *Hydrobiologia*, 802(1), 71–83.
576 <https://doi.org/10.1007/s10750-017-3240-1>
- 577 Mcleod, E., Chmura, G. L., Bouillon, S., Salm, R., Björk, M., Duarte, C. M., Lovelock, C. E.,
578 Schlesinger, W. H., & Silliman, B. R. (2011). A blueprint for blue carbon: Toward an improved
579 understanding of the role of vegetated coastal habitats in sequestering CO₂. *Frontiers in Ecology*
580 *and the Environment*, 9(10), 552–560. <https://doi.org/10.1890/110004>
- 581 Megonigal, J. P., Whalen, S. C., Tissue, D. T., Bovard, B. D., Allen, A. S., & Albert, D. B. (1999). A
582 Plant-Soil-Atmosphere Microcosm for Tracing Radiocarbon from Photosynthesis through
583 Methanogenesis. *Soil Science Society of America Journal*, 63(3), 665–671.
584 <https://doi.org/10.2136/sssaj1999.03615995006300030033x>
- 585 Megonigal, J. Patrick, Chapman, S., Crooks, S., Dijkstra, P., Kirwan, M., & Langley, A. (2016). 3.4
586 Impacts and effects of ocean warming on tidal marsh and total freshwater forest ecosystems. In
587 D. Laffoley & J. M. Baxter (Eds.), *Explaining Ocean Warming: Causes, scale, effects, and*
588 *consequences*. IUCN.
- 589 Megonigal, J. Patrick, Hines, M. E., & Visscher, P. T. (2004). Anaerobic metabolism: Linkages to trace
590 gases and aerobic processes. In W. H. Schlesinger (Ed.), *Biogeochemistry* (pp. 317–424).
591 Elsevier-Pergamon.
- 592 Megonigal, J. Patrick, & Schlesinger, William. H. (2002). Methane-limited methanotrophy in tidal
593 freshwater swamps. *Global Biogeochemical Cycles*, 16(4), 1088.
594 <https://doi.org/10.1029/2001GB001594>
- 595 Moor, H., Rydin, H., Hylander, K., Nilsson, M. B., Lindborg, R., & Norberg, J. (2017). Towards a trait-
596 based ecology of wetland vegetation. *Journal of Ecology*, 105(6), 1623–1635.
597 <https://doi.org/10.1111/1365-2745.12734>
- 598 Mueller, P., Jensen, K., & Megonigal, J. P. (2016). Plants mediate soil organic matter decomposition in



- 599 response to sea level rise. *Global Change Biology*, 22(1), 404–414.
- 600 <https://doi.org/10.1111/gcb.13082>
- 601 Mueller, P., Mozdzer, T. J., Langley, J. A., Aoki, L. R., Noyce, G. L., & Megonigal, J. P. (in press).
- 602 Plants determine methane response to sea level rise. *Nature Communications*.
- 603 <https://doi.org/10.1038/s41467-020-18763-4>
- 604 Neubauer, S. C., Emerson, D., & Megonigal, J. P. (2008). Microbial oxidation and reduction of Iron in
- 605 the root zone and influences on metal mobility. In *Biophysico-Chemical Processes of Heavy*
- 606 *Metals and Metalloids in Soil Environments* (pp. 339–371). John Wiley & Sons, Ltd.
- 607 <https://doi.org/10.1002/9780470175484.ch9>
- 608 Neubauer, Scott C., & Craft, C. B. (2009). Chapter 23 Global Change and Tidal Freshwater Wetlands:
- 609 Scenarios and Impacts. In A. Barendregt, D. Whigham, & A. Baldwin (Eds.), *Tidal Freshwater*
- 610 *Wetlands* (pp. 253–310). Margraf Publishers.
- 611 Neubauer, Scott C., & Megonigal, J. P. (2015). Moving beyond global warming potentials to quantify the
- 612 climatic role of ecosystems. *Ecosystems*, 18(6), 1000–1013. [https://doi.org/10.1007/s10021-015-](https://doi.org/10.1007/s10021-015-9879-4)
- 613 [9879-4](https://doi.org/10.1007/s10021-015-9879-4)
- 614 Noyce, G. L., Kirwan, M. L., Rich, R. L., & Megonigal, J. P. (2019). Asynchronous nitrogen supply and
- 615 demand produce non-linear plant allocation responses to warming and elevated CO₂. *Proceedings*
- 616 *of the National Academy of Sciences*.
- 617 Pastore, M. A., Megonigal, J. P., & Langley, J. A. (2017). Elevated CO₂ and nitrogen addition accelerate
- 618 net carbon gain in a brackish marsh. *Biogeochemistry*, 133(1), 73–87.
- 619 <https://doi.org/10.1007/s10533-017-0312-2>
- 620 Pendleton, L., Donato, D. C., Murray, B. C., Crooks, S., Jenkins, W. A., Sifleet, S., Craft, C., Fourqurean,
- 621 J. W., Kauffman, J. B., Marbà, N., Megonigal, P., Pidgeon, E., Herr, D., Gordon, D., & Baldera,
- 622 A. (2012). Estimating global “blue carbon” emissions from conversion and degradation of
- 623 vegetated coastal ecosystems. *PLOS ONE*, 7(9), e43542.
- 624 <https://doi.org/10.1371/journal.pone.0043542>



- 625 Philippot, L., Hallin, S., Börjesson, G., & Baggs, E. M. (2009). Biochemical cycling in the rhizosphere
626 having an impact on global change. *Plant and Soil*, 321(1), 61–81.
627 <https://doi.org/10.1007/s11104-008-9796-9>
- 628 Poffenbarger, H. J., Needelman, B. A., & Megonigal, J. P. (2011). Salinity influence on methane
629 emissions from tidal marshes. *Wetlands*, 31(5), 831–842. [https://doi.org/10.1007/s13157-011-](https://doi.org/10.1007/s13157-011-0197-0)
630 0197-0
- 631 Rich, R. L., Stefanski, A., Montgomery, R. A., Hobbie, S. E., Kimball, B. A., & Reich, P. B. (2015).
632 Design and performance of combined infrared canopy and belowground warming in the
633 B4WarmED (Boreal Forest Warming at an Ecotone in Danger) experiment. *Global Change*
634 *Biology*, 21(6), 2334–2348. <https://doi.org/10.1111/gcb.12855>
- 635 Robroek, B. J. M., Albrecht, R. J. H., Hamard, S., Pulgarin, A., Bragazza, L., Buttler, A., & Jassey, V. E.
636 (2016). Peatland vascular plant functional types affect dissolved organic matter chemistry. *Plant*
637 *and Soil*, 407(1), 135–143. <https://doi.org/10.1007/s11104-015-2710-3>
- 638 Saunio, M., Bousquet, P., Poulter, B., Peregón, A., Ciais, P., Canadell, J. G., Dlugokencky, E. J., Etiope,
639 G., Bastviken, D., Houweling, S., Janssens-Maenhout, G., Tubiello, F. N., Castaldi, S., Jackson,
640 R. B., Alexe, M., Arora, V. K., Beerling, D. J., Bergamaschi, P., Blake, D. R., ... Peng, S. (2016).
641 The global methane budget 2000-2012. *Earth System Science Data*, 8(2), 697–751.
642 <http://dx.doi.org/10.5194/essd-8-697-2016>
- 643 Segers, R. (1998). Methane production and methane consumption: A review of processes underlying
644 wetland methane fluxes. *Biogeochemistry*, 41(1), 23–51.
645 <https://doi.org/10.1023/A:1005929032764>
- 646 Sihi, D., Inglett, P. W., Gerber, S., & Inglett, K. S. (2017). Rate of warming affects temperature
647 sensitivity of anaerobic peat decomposition and greenhouse gas production. *Global Change*
648 *Biology*, 24(1), e259–e274. <https://doi.org/10.1111/gcb.13839>
- 649 Sorrell, B. K., Brix, H., Schierup, H.-H., & Lorenzen, B. (1997). Die-back of *Phragmites australis*:
650 Influence on the distribution and rate of sediment methanogenesis. *Biogeochemistry*, 36(2), 173–
29



- 651 188. <https://doi.org/10.1023/A:1005761609386>
- 652 Stanley, E. H., & Ward, A. K. (2010). Effects of Vascular Plants on Seasonal Pore Water Carbon
653 Dynamics in a Lotic Wetland. *Wetlands*, 30(5), 889–900. <https://doi.org/10.1007/s13157-010->
654 0087-x
- 655 Sutton-Grier, Ariana. E., Keller, J. K., Koch, R., Gilmour, C., & Megonigal, J. P. (2011). Electron donors
656 and acceptors influence anaerobic soil organic matter mineralization in tidal marshes. *Soil*
657 *Biology and Biochemistry*, 43(7), 1576–1583. <https://doi.org/10.1016/j.soilbio.2011.04.008>
- 658 van Bodegom, P. M., & Stams, A. J. M. (1999). Effects of alternative electron acceptors and temperature
659 on methanogenesis in rice paddy soils. *Chemosphere*, 39(2), 167–182.
660 [https://doi.org/10.1016/S0045-6535\(99\)00101-0](https://doi.org/10.1016/S0045-6535(99)00101-0)
- 661 van der Nat, F.-J., & Middelburg, J. J. (1998). Effects of two common macrophytes on methane dynamics
662 in freshwater sediments. *Biogeochemistry*, 43(1), 79–104.
663 <https://doi.org/10.1023/A:1006076527187>
- 664 van der Nat, F.-J. W. A., & Middelburg, J. J. (1998). Seasonal variation in methane oxidation by the
665 rhizosphere of *Phragmites australis* and *Scirpus lacustris*. *Aquatic Botany*, 61(2), 95–110.
666 [https://doi.org/10.1016/S0304-3770\(98\)00072-2](https://doi.org/10.1016/S0304-3770(98)00072-2)
- 667 van Hulzen, J. B., Segers, R., van Bodegom, P. M., & Leffelaar, P. A. (1999). Temperature effects on soil
668 methane production: An explanation for observed variability. *Soil Biology and Biochemistry*,
669 31(14), 1919–1929. [https://doi.org/10.1016/S0038-0717\(99\)00109-1](https://doi.org/10.1016/S0038-0717(99)00109-1)
- 670 Vann, C. D., & Megonigal, J. P. (2003). Elevated CO₂ and water depth regulation of methane emissions:
671 Comparison of woody and non-woody wetland plant species. *Biogeochemistry*, 63(2), 117–134.
672 <https://doi.org/10.1023/A:1023397032331>
- 673 Waldo, N. B., Hunt, B. K., Fadely, E. C., Moran, J. J., & Neumann, R. B. (2019). Plant root exudates
674 increase methane emissions through direct and indirect pathways. *Biogeochemistry*, 145(1), 213–
675 234. <https://doi.org/10.1007/s10533-019-00600-6>
- 676 Ward, S. E., Ostle, N. J., Oakley, S., Quirk, H., Henrys, P. A., & Bardgett, R. D. (2013). Warming effects



677 on greenhouse gas fluxes in peatlands are modulated by vegetation composition. *Ecology Letters*,
678 16(10), 1285–1293. <https://doi.org/10.1111/ele.12167>

679 Wassmann, R., Alberto, M. C., Tirol-Padre, A., Hoang, N. T., Romasanta, R., Centeno, C. A., & Sander,
680 B. O. (2018). Increasing sensitivity of methane emission measurements in rice through
681 deployment of ‘closed chambers’ at nighttime. *PLOS ONE*, 13(2), e0191352.
682 <https://doi.org/10.1371/journal.pone.0191352>

683 Weston, N. B., & Joye, S. B. (2005). Temperature-driven decoupling of key phases of organic matter
684 degradation in marine sediments. *Proceedings of the National Academy of Sciences of the United*
685 *States of America*, 102(47), 17036–17040. <https://doi.org/10.1073/pnas.0508798102>

686 Wilson, R. M., Hopple, A. M., Tfaily, M. M., Sebestyen, S. D., Schadt, C. W., Pfeifer-Meister, L.,
687 Medvedeff, C., McFarlane, K. J., Kostka, J. E., Kolton, M., Kolka, R. K., Kluber, L. A., Keller, J. J.,
688 K., Guilderson, T. P., Griffiths, N. A., Chanton, J. P., Bridgham, S. D., & Hanson, P. J. (2016).
689 Stability of peatland carbon to rising temperatures. *Nature Communications*, 7, ncomms13723.
690 <https://doi.org/10.1038/ncomms13723>

691 Yang, P., Wang, M. H., Lai, D. Y. F., Chun, K. P., Huang, J. F., Wan, S. A., Bastviken, D., & Tong, C.
692 (2019). Methane dynamics in an estuarine brackish *Cyperus malaccensis* marsh: Production and
693 porewater concentration in soils, and net emissions to the atmosphere over five years. *Geoderma*,
694 337, 132–142. <https://doi.org/10.1016/j.geoderma.2018.09.019>

695 Ye, R., Jin, Q., Bohannon, B., Keller, J. K., & Bridgham, S. D. (2014). Homoacetogenesis: A potentially
696 underappreciated carbon pathway in peatlands. *Soil Biology and Biochemistry*, 68(Supplement
697 C), 385–391. <https://doi.org/10.1016/j.soilbio.2013.10.020>

698 Yvon-Durocher, G., Allen, A. P., Bastviken, D., Conrad, R., Gudas, C., St-Pierre, A., Thanh-Duc, N., &
699 del Giorgio, P. A. (2014). Methane fluxes show consistent temperature dependence across
700 microbial to ecosystem scales. *Nature*, 507(7493), 488–491. <https://doi.org/10.1038/nature13164>
701